An approach to classification and under-sampling of the interfering wireless signals

Andjela Draganić, Irena Orović, Srdjan Stanković, Xiumei Li, Zhi Wang

Abstract*—Classification of interfering signals that belong todifferent wireless standards is important topic in wireless communications. In this paper, we propose a procedure for separation and classification of wireless signals belonging to the Bluetooth and to the IEEE 802.11b standards. These signals operate in the same frequency band and may interfere with each other. The procedure is made of a few steps. In the first step, the separation of signal components is done using the eigenvalue decomposition approach. The second stage is based on the compressive sensing approach, used to reduce the number of transmitted samples. A suitable transform domain is chosen for each separated component using ℓ_1-norm as a measure of sparsity. Since the Bluetooth signals are less sparse compared to the IEEE 802.11b signals, after choosing sparse domain, additional sparsification needs to performed to further enhance the sparsity. In the last step of the procedure, the classification is performed by observing the time-frequency characteristics of the reconstructed separated components. The theory is proved by the experimental results.

***Keywords* - Compressive Sensing, Eigenvalue Decomposition, FHSS signals, IEEE 802.11b, signal separation**

I. Introduction

Depending on the system requirements, wireless standards differ in data rates, energy consumption, signal modulations, operation distances, etc. [1]-[4]. Low power consumption and high speed transmission are desirable in all existing standards. Also, securing information transmission is of great importance in wireless technology. Therefore, the spread spectrum modulation is commonly applied modulation technique in communications, since it provides robustness to jamming, inter-symbol interference (ISI), noise and robustness to other environmental factors [1]-[4]. Spread spectrum modulations spread the frequency spectrum of a data-signal by using a code, unique for every user and uncorrelated with the observed signal. This results in much higher bandwidth occupancy than it is required.

Two types of spread spectrum modulations are observed in this paper: direct sequence spread spectrum (DSSS) and frequency hopping spread spectrum (FHSS), due to their applications in two interfering wireless standards. First modulation technique is used in IEEE 802.11b standard for wireless LAN [2]. It causes phase transitions in the carrier data by applying the fast pseudorandom sequence. The second technique is used in Bluetooth standard and is also based on the carrier frequency shifting in a pseudorandom way [2].

These two standards are of particular interest because they share the same operation frequency band - Industrial, Scientific and Medical (ISM) band. Therefore, the interferences between the two types of signals are common. Also, both standards deal with the sinusoidal signals, but with different physical characteristics of their components. Namely, the FHSS signal has short duration components, while the components of the IEEE 802.11b signal have longer time duration. The physical characteristics of components will be exploited for classification [2], [5]-[7] after components separation is done by applying the eigenvalue decomposition (EVD).

The EVD [8]-[13] has numerous practical applications, including image analysis and signal processing, for characterization of signals and their components [9]. In this paper the EVD is applied to separate components of multicomponent signal belonging to different wireless standards. As a result, the eigenvectors corresponding to the separated components are obtained [6]. Then the eigenvectors are under-sampled in order to decrease the amount of transmitted data and to increase the transmission efficiency. At the receiver side, the eigenvectors are represented in the time-frequency domain to determine the physical features used for classification of components.

In the light of Compressive Sensing (CS) theory, only a small number of randomly selected samples per eigenvector are chosen to be sent through the communication channel. At the receiver side, all signal components need to be completely reconstructed from transmitted samples, where the reconstruction is performed by using complex mathematical algorithms. An important requirement for successful reconstruction of CS-based eigenvectors is the sparsity property [14]-[20]. This property is achieved in the transform domain where the signal information is concentrated into few coefficients [21]-[23]. In order to provide sparsity for both considered signal types, the transform domain selection is used as a special step in the proposed procedure. Due to the nature of the observed signal types, the choice is made between the discrete Fourier transform (DFT) and the Hermite transform (HT) domain [23]-[28]. The optimization of the HT parameters is applied to increase the sparsity of components [27].

The paper is structured as follows: Section II provides theoretical background on the EVD used for components separation. Section III focuses on CS approach and sparse domain selection, while the proposed procedure is summarized and described in the Section IV. Experimental evaluation is provided in Section V. The concluding remarks are given in Section VI.

II. THEORETICAL BACKGROUND

The EVD [9]-[12] is a method used to decompose high-dimensional signals into approximately decorrelated components. In other words, EVD finds the directions of maximum variations in the data [29], and project the data onto these directions. Directions with the most variations correspond to the eigenvectors related to the largest eigenvalues of the covariance matrix. For a certain covariance matrix **R**, the EVD is defined as follows [9]:

$$\mathbf{R} = \mathbf{U}\Lambda\mathbf{U}^{\mathbf{T}} = \sum_{i=1}^{N+1} \lambda_i u_i(n) u^*_i(n), \tag{1}$$

where **U** is an eigenvectors matrix, $\mathbf{\Lambda}$ is a diagonal eigenvalues matrix where eigenvalues are sorted in decreasing order, λ_i are eigenvalues and u_i are eigenvectors. Here, the covariance matrix is defined based on the TF autocorrelation matrix. The EVD of this matrix produces eigenvectors that correspond to the signals components, while the eigenvalues correspond to their energy [8],[9].

If a monocomponent signal $x(n)$ is observed, the autocorrelation matrix can be defined as:

$$\mathbf{R} = x(n)x^*(n), \tag{2}$$

where $x^*(n)$ denotes complex conjugate of the vector $x(n)$. By summing up the right side of (2), the autocorrelation matrix for K-component signal is obtained:

$$\mathbf{R_K} = \sum_{i=1}^{K} x_i(n) x_i^*(n). \tag{3}$$

The right side of (3) can be defined by using the inverse form of the Wigner distribution:

$$\sum_{i=1}^{K} x_i(n+m) x_i^*(n-m) = \frac{1}{N+1} \sum_{k=-N/2}^{N/2} \sum_{i=1}^{K} WD_i(n,k) e^{j\frac{2\pi}{N+1}2mk}, \tag{4}$$

where N is the signal length, WD denotes the Wigner distribution $WD(n,k) = \sum_{m=-N/2}^{N/2} x(n+m)x^*(n-m)e^{-j\frac{2\pi}{N+1}2mk}$, and m is time shift.

If there is no overlapping in the TF plane, the sum of Wigner distributions of signal components is equal to the S-method of the multicomponent signal. Therefore, (4) can be modified as follows [8],[9]:

$$\sum_{i=1}^{K} x_i(n+m)x_i^*(n-m) = \frac{1}{N+1}\sum_{k=-N/2}^{N/2} SM(n,k)e^{j\frac{4\pi}{N+1}mk}, \tag{5}$$

where SM denotes the S-method. In other words,

$$R_K(n+m,n-m) = \frac{1}{N+1}\sum_{k=-N/2}^{N/2} SM(n,k)e^{j\frac{4\pi}{N+1}mk}, \tag{6}$$

where $\mathbf{R_K}$ is a square autocorrelation matrix. Then, the EVD of the square matrix $\mathbf{R_K}$ could be written as:

$$\mathbf{R_K} = \sum_{i=1}^{N+1} \lambda_i u_i(n)u^*_i(n), \tag{7}$$

resulting in eigenvalues and eigenvectors that will correspond to the signal components.

III. A CS APPROACH AND SPARSE DOMAIN SELECTION

In order to decrease the amount of data transmitted through the communication channel, the eigenvectors are randomly under-sampled by applying the compressive sensing paradigm. Along with a random selection of signal samples that will guarantee incoherence, sparsity is another required CS condition. The sparsity means that majority of the coefficients are zeros (or negligible) in certain transform domain, i.e., the signal information is condensed into a small number of non-zero coefficients. Depending on the signal nature and required reconstruction accuracy, different algorithms can be used for recovering under-sampled sparse signals [16]-[20].

Let us now describe the procedure for obtaining CS-based eigenvectors. If the discrete eigenvector $\mathbf{u}$ of length N is sparse in the transform domain $\mathbf{\Psi}$, it can be represented in terms of basis vectors as follows:

$$\mathbf{u} = \sum_{i=1}^{N} \mathbf{U}_i \psi_i = \mathbf{\Psi U}, \tag{8}$$

where $\mathbf{U}$ denotes transform domain coefficients of the eigenvector (where only $S<<N$ coefficients are non-zero). By introducing the matrix $\mathbf{\Theta}$, that models random samples selections from the starting eigenvector, the vector of available measurements $\mathbf{y}$ (of length $M_a<N$) can be defined as:

$$\mathbf{y} = \mathbf{\Theta \Psi U}. \tag{9}$$

The system of equations (9) is undetermined, since the number of available samples M_a is smaller than the total number of samples N. In order to obtain a unique solution, the optimization algorithms are used such as greedy ones (e.g. OMP, CoSaMP), thresholding algorithms (e.g. IHT, IST), Automated Threshold Based Iterative Solution, Adaptive Gradient-Based Algorithm, etc. [16]-[20].

Sparse transform domain selection

Having in mind that the DSSS modulated components by their nature correspond to the full-time duration sinusoids, the DFT domain is suitable to reveal the sparsity. On the other side, the FHSS signals are characterized by short-duration sinusoidal components, producing spectrum leakage around in the DFT domain, thus ruining sparsity. Moreover, due to the shape similarity between the FHSS components and Hermite functions, we may conclude that the Hermite transform (HT) is more suitable choice compared to DFT. Hence, the decision on the sparsity domain is made by measuring the concentration using the ℓ_1-norm:

$$\|\mathbf{U}\|_{\ell_1} = \sum_{n=0}^{N-1} |U(n)|, \quad \mathbf{U} = \mathbf{\Psi}^{-1}\mathbf{u}, \tag{10}$$

where $\mathbf{\Psi}^{-1}$ can be either DFT or HT matrix. Discrete Hermite function of an order p is defined as [23]-[27]:

$$\psi_p(t_m) = \frac{e^{-t_m^2} H_p\left(t_m / \sigma\right)}{\sqrt{\sigma 2^p\, p!\sqrt{\pi}}}\ , \tag{11}$$

while HT matrix can be defined as:

$$\Psi = \frac{1}{M}\begin{bmatrix} \frac{\psi_0(t_1)}{(\psi_{M-1}(t_1))^2} & \cdots & \frac{\psi_0(t_M)}{(\psi_{M-1}(t_M))^2} \\ \frac{\psi_1(t_1)}{(\psi_{M-1}(t_1))^2} & \cdots & \frac{\psi_1(tM)}{(\psi_{M-1}(t_M))^2} \\ \cdots & \cdots & \cdots \\ \frac{\psi_{M-1}(t_1)}{(\psi_{M-1}(t_1))^2} & \cdots & \frac{\psi_{M-1}(t_M)}{(\psi_{M-1}(t_M))^2} \end{bmatrix}, \tag{12}$$

and its inverse form:

$$\Psi^{-1} = \begin{bmatrix} \psi_0(t_1) & \cdots & \psi_{M-1}(t_1) \\ \psi_0(t_2) & \cdots & \psi_{M-1}(t_2) \\ \cdots & \cdots & \cdots \\ \psi_0(t_M) & \cdots & \psi_{M-1}(t_M) \end{bmatrix}. \tag{13}$$

The parameter M denotes the number of Hermite functions used to represent the signal, i.e. M is the order of the Hermite polynomial. The H_p denotes the Hermite polynomial whose zeros are t_m. The factor σ is a scaling factor and it is used to stretch and compress the Hermite functions. This means that each function can be adapted to the observed signal which will provide an additional sparsification.

When applying the HT, the eigenvectors of length N should be resampled at non-uniform points being proportional to the roots of the N-th order Hermite polynomial. For that purpose, *sinc* interpolation function can be used to obtain the values at the requested non-uniform points as follows:

$$u(\lambda t_m) \approx \sum_{n=-N/2}^{N/2} u(n\Delta t) \frac{\sin\left(\pi(\lambda t_m - n\Delta t)/\Delta t\right)}{\pi(\lambda t_m - n\Delta t)/\Delta t}, \tag{14}$$

where m = 1,…,N, Δt is the sampling period and is time-axis scaling factor, that is used instead of σ. In order to improve the sparsity, the procedure for the optimization of λ is employed. The concentration measure based on the ℓ_1-norm is used to find the value of λ producing the lowest sparsity:

$$\lambda_{opt} = \min_{\lambda} \left\| U(\lambda t_m) \right\|_{\ell_1} = \left\| \mathrm{HT}\left\{ \sum_{n=-N/2}^{N/2} u(n\Delta t) \frac{\sin\left(\pi(\lambda t_m - n\Delta t)/\Delta t\right)}{\pi(\lambda t_m - n\Delta t)/\Delta t} \right\} \right\|_1 . \tag{15}$$

IV. A CS-BASED WIRELESS SIGNALS CLASSIFICATION PROCEDURE

The procedure aimed to separate and classify the components of the interfering Bluetooth and IEEE 802.11b signals is summarized in the sequel. It is consisted of six steps, and based on the previously described EVD and CS approaches.

A. First the TF representation of the input signal is calculated using the S-method that provides good concentration of auto components and avoids cross terms in the observed multicomponent signals. The S-method calculation is based on the short-Time Fourier transform (STFT):

$$STFT(n,k) = \sum_{m=-N/2}^{N/2-1} w(m)x(n+m)e^{-j2\pi mk/N}, \tag{16}$$

where $x(n)$ is an input signal and $w(n)$ is a sliding window.

Then the S-method can be calculated as:

$$SM(n,k) = \sum_{i=-L}^{L} STFT(n,k+i)STFT^{*}(n,k-i), \tag{17}$$

where the parameter L usually takes values between 3 and 6.

B. Next, the autocorrelation matrix $\mathbf{R_K}$ used in the EVD, is calculated as an inverse of the S-method, according to (6).

C. The choice of sparsity domain is done by measuring the concentrations of the DFT and HT for each eigenvector, based on the ℓ_1-norm and according to (10).

D. The next step assumes random under-sampling of the eigenvectors, which is done by simply selecting certain percent of random samples.

Inputs:

- ♦ Signal $\boldsymbol{x}$
- ♦ Window function for STFT calculation $\boldsymbol{w}$
- ♦ S-method window width L

A. Calculate the STFT and the S-method of the signal $\boldsymbol{x}$:

$$STFT(n,k)=\sum_{m=-N/2}^{N/2-1} w(m)x(n+m)e^{-j2\pi mk/N}$$

$$SM(n,k)=\sum_{i=-L}^{L} STFT(n,k+i)STFT^{*}(n,k-i)$$

B. Calculate the TF based autocorrelation matrix and perform EVD:

$$\mathbf{R}_{\mathbf{K}}=inv(SM),\quad \text{EVD}\{\mathbf{R}_{\mathbf{K}}\}\rightarrow\sum_{i=1}^{N+1}\lambda_i u_i(n)u^{*}_i(n)$$

C. Choose sparsification domain for each eigenvector $\mathbf{u_i}$.
Measuring the HT and DFT ℓ_1-norm concentration:

$$\|\mathbf{U}\|_{\ell_1}^{H}=\sum_{n=0}^{N-1}|U_H(n)|,\ \ \mathbf{U}_H=\mathbf{\Psi}^{-1}\mathbf{u}\qquad (\Psi \text{ denotes HT matrix})$$

$$\|\mathbf{U}\|_{\ell_1}^{F}=\sum_{n=0}^{N-1}|U_F(n)|,\ \ \mathbf{U}_F=\mathbf{\Psi}^{-1}\mathbf{u}\qquad (\Psi \text{ denotes DFT matrix})$$

- If $\|\mathbf{U}\|_{\ell_1}^{H}>\|\mathbf{U}\|_{\ell_1}^{F}\Rightarrow\mathbf{\Psi}^{-1}\rightarrow$ DFT matrix. Go to step **D**.
- If $\|\mathbf{U}\|_{\ell_1}^{H}<\|\mathbf{U}\|_{\ell_1}^{F}\Rightarrow\mathbf{\Psi}^{-1}\rightarrow$ HT matrix. HT optimization:

-eigenvector *sinc* interpolation:

$$u(\lambda t_m)\approx\sum_{n=-N/2}^{N/2}u(n\Delta t)\frac{\sin\left(\pi(\lambda t_m-n\Delta t)/\Delta t\right)}{\pi(\lambda t_m-n\Delta t)/\Delta t}$$

- finding optimal time-scaling factor:

$$\lambda_{opt}=\min_{\lambda}\|U(\lambda t_m)\|_{\ell_1}=$$

$$=\left\|\text{HT}\left\{\sum_{n=-N/2}^{N/2}u(n\Delta t)\frac{\sin\left(\pi(\lambda t_m-n\Delta t)/\Delta t\right)}{\pi(\lambda t_m-n\Delta t)/\Delta t}\right\}\right\|_{\ell_1}$$

D. Random under-sampling of eigenvectors.

$\mathbf{y}=\Theta\Psi\mathbf{U}$ (domain of sparsity Ψ chosen in **C**.)

E. Under-sampled eigenvectors reconstruction:

$\widehat{\text{U}}=\min\|\mathbf{U}\|_{\ell_1}=\sum_{i=1}^{N}|\text{U}_i|$ subject to $\mathbf{y}=\Theta\Psi\mathbf{U}$

F. S-method calculation for the reconstructed eigenvectors and their classification

Outputs:

- FHSS signal: $x_{FHSS}(t)=\sum u_{FHSS}(t)$
- DSSS signal: $x_{DSSS}(t)=\sum u_{DSSS}(t)$

Figure 1. The algorithm for components separation and classification based on the EVD and CS approach

E. After transmission, the vectors are reconstructed by using the optimization algorithms. Here, the ℓ_1-norm minimization is used for the vector reconstruction:

$$\widehat{\mathbf{U}}=\min\|\mathbf{U}\|_{\ell_1}\qquad\text{subject to}\quad \mathbf{y}=\Theta\Psi\mathbf{U}\ . \tag{18}$$

The solution of the ℓ_1 minimization problem is based on the basis pursuit primal-dual, and performed by using the L1-magic solver.

F. Finally, the S-method is calculated for each individual reconstructed eigenvector. Then the eigenvector features in the TF plane are used to make decision about the specific component type (related to the communication standard). The whole procedure is described in the Figure 1 diagram.

The proposed procedure does not require the a priori knowledge of the components' frequencies. Hence, the procedure provides blind sinusoidal components separation belonging to different frequencies, as long as there are no overlapping and intersections between components in time or in frequency. The FHSS and DSSS modulations use different frequency channels in the ISM frequency band. FHSS components appear over 79 channels, while DSSS modulation uses 14 channels. Therefore, intersections and overlapping do not appear between the components belonging to different signals.

Regarding the energies of the signal components, it is important to note that the eigenvalues λ_i, that are result of the EVD procedure, correspond to the energies of the signal components. The greatest eigenvalue will correspond to the first eigenvector, i.e. the strongest signal component, while the second one will correspond to the second greatest component, and so on. Therefore, the strongest component will be extracted at the first place, followed by the components that have lower energy.

V. EXPERIMENTAL RESULTS

The proposed procedure is tested on synthetic signal. Signal contains both interfering standards: signal belongs to the Bluetooth standard and the IEEE 802.11b standard. The signal length is 256 samples and contains seven components: four components are FHSS modulated, while three components are DSSS modulated.
The S-method of the combined signal is shown in Figure 2.

We may observe that the Bluetooth signal components have higher energy compared to the components of the IEEE 802.11b signal. Therefore, the first four eigenvectors obtained from the EVD will correspond to the components of higher energy, i.e., components of the Bluetooth signal, while the 5th, 6th and 7th eigenvectors will correspond to the IEEE 802.11b components.

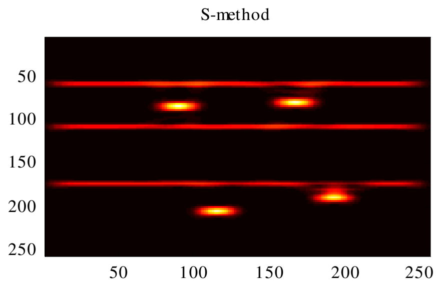

Figure 2. The S-method of the original signal; *x*-axis is time, *y*-axis is frequency

After the eigenvectors are obtained, the sparsity domain is chosen for each of them, based on the ℓ_1-norm sparsity measure. The values of the concentration measure for 7 observed eigenvectors are given in Table 1. Also, for the first four eigenvectors we provide their DFTs and optimized HTs in in Figure 3a. Both transform domains are plotted in order to illustrate that the HT provides better sparsity compared to DFT for the FHSS components. The last three eigenvectors are illustrated in the DFT as a dominant sparsity domain, Figure 3b.

Table 1: Eigenvectors concentration measures calculated for both, HT and DFT domains

Eigenvector No	*Sparsity measure-Hermite transform*	*Sparsity measure-Fourier transform*	*Sparsity domain*
1	**27.9601**	37.3387	***HT***
2	**28.4100**	36.2452	***HT***
3	**32.7542**	41.4611	***HT***
4	**27.8796**	37.4397	***HT***
5	68.2208	**22.9848**	***DFT***
6	67.7154	**19.7623**	***DFT***
7	94.0820	**25.4799**	***DFT***

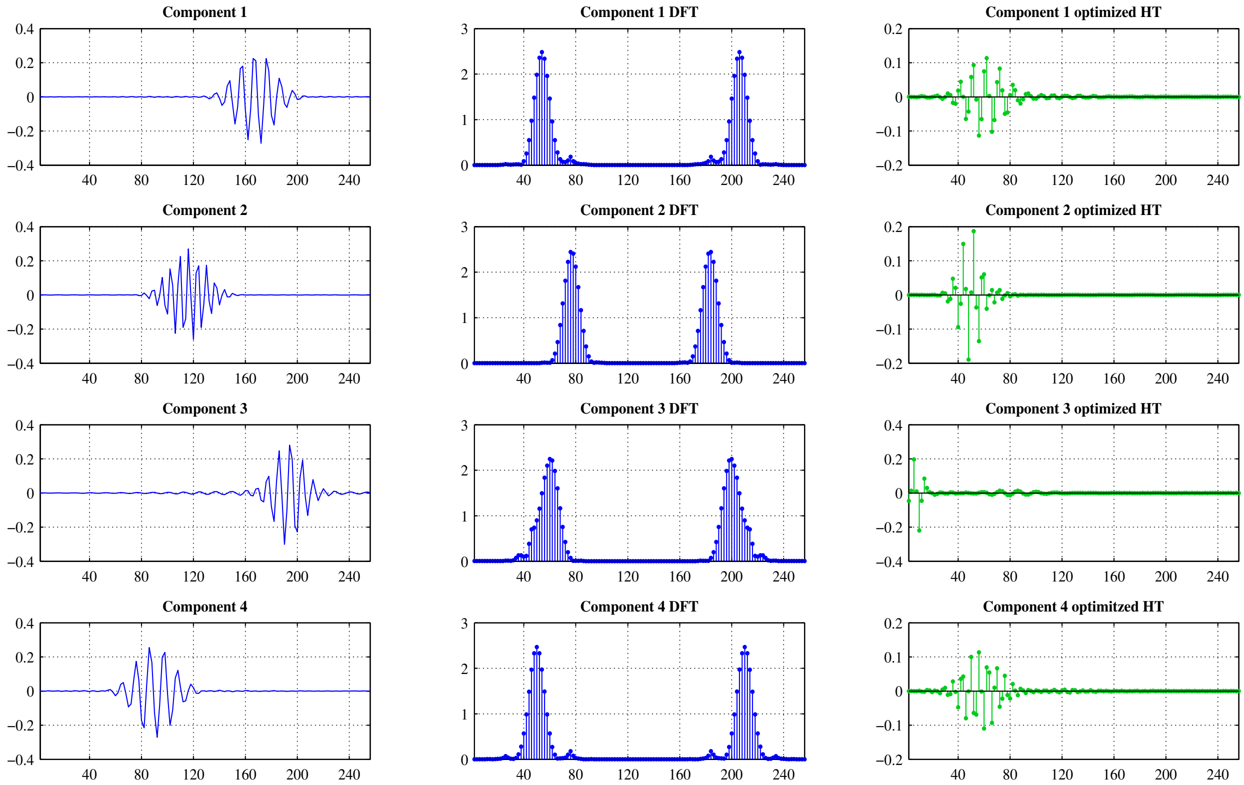

a)

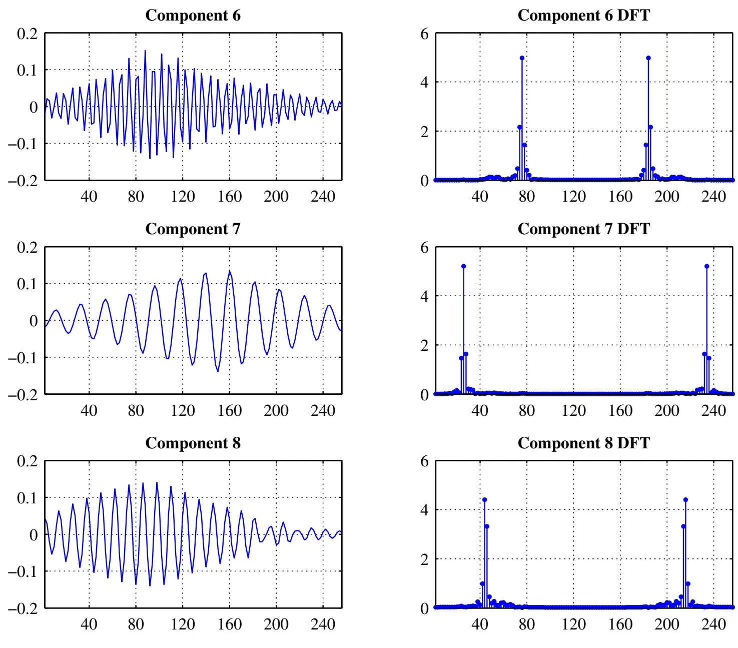

b)

Figure 3. a) First 4 eigenvectors (first column, *x*-axis is time, *y*-axis is amplitude) and their corresponding DFTs (second column, *x*-axis is frequency, *y*-axis is amplitude); Optimized HTs for the first 4 eigenvectors (third column, *x*-axis denotes order of the Hermite coefficient, *y*-axis is amplitude); b) 5^{th}, 6^{th} and 7^{th} eigenvector (first column, *x*-axis is time, *y*-axis is amplitude) and their DFTs (second column, *x*-axis is frequency, *y*-axis is amplitude);

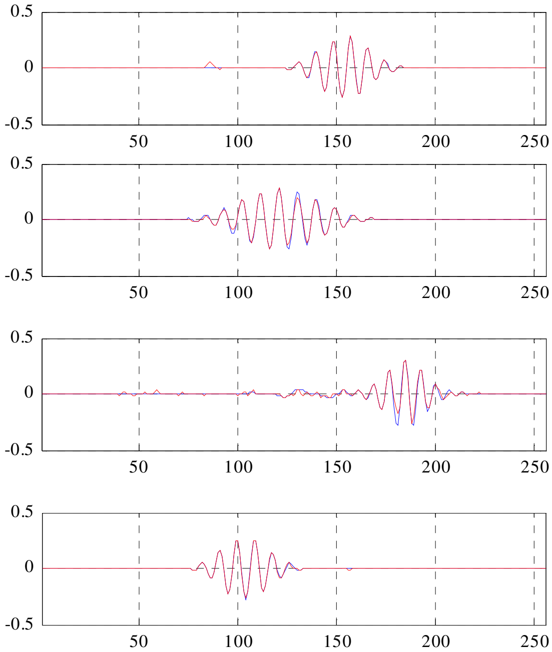

Figure 4. Separated components of the Bluetooth signal – blue is the original component, red is the CS reconstructed component. The percent of the randomly selected samples is 45% (*x*-axis is time, *y*-axis is amplitude)

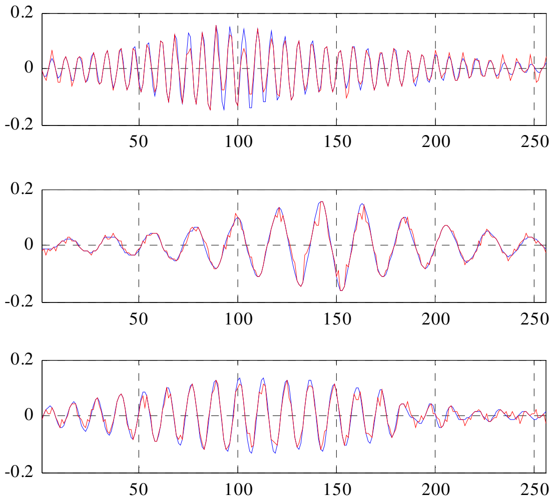

Figure 5. Separated components of the IEEE 802.11b signal – blue is the original component, red is the CS reconstructed component. The percent of the randomly selected samples is 45% (*x*-axis is time, *y*-axis is amplitude)

Based on the sparsity measure, HT is chosen as sparse domain for the first four eigenvectors, while DFT is chosen for the three remaining eigenvectors. After selecting the transform domain, the HTs of the corresponding eigenvectors are additionally optimized in order to improve the sparsity as described in Section III.

The obtained eigenvectors are randomly under-sampled to be transmitted with lower amount of data. Only 45% of the total number of samples is chosen from each eigenvector. At the receiver side, the eigenvectors' reconstruction is done by using basis pursuit primal-dual reconstruction algorithm. The original (blue) and reconstructed (red) eigenvectors are shown in Figures 4 and 5: FHSS modulated components are shown in Figure 4, while DSSS modulated components are shown in Figure 5. The last step is the calculation of TFR for the reconstructed components. The S-methods of the separated signal components are shown in Figure 6.

Classification of the signal components is done here by observing the TF representations of each separated component. The time durations of the components are extracted from the TF representation, and based on their values, the classification to the Bluetooth or IEEE 802.11b standard is done. The features extraction and signal classification based on the TF representations, is proposed in [2]. The durations of the separated components, estimated from the components S-methods, are given in the Table 2. As it can be seen, the FHSS components has shorter duration compared to the IEEE 802.11b signal components. The reconstruction errors are provided within the Table 3. The mean square error (MSE) between original and reconstructed eigenvector is observed.

Note that components classification can also be done in the step **C.** of the algorithm, based on the value of the concentration measure. In the case of HT domain, the FHSS signal components will have lower concentration measure compared to the IEEE 802.11b signal components.

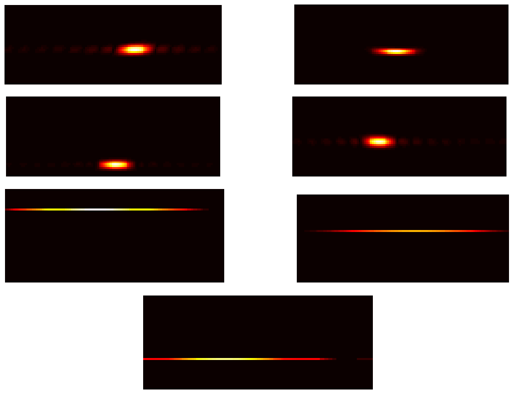

Figure 6. S-method of the separated components: first 4 figures correspond to the S-method of the FHSS modulated signal, while remaining 3 figures correspond to the S-method of the DSSS modulated signal (x-axis is time, y-axis is frequency)

Table 2: Components duration, estimated from the TF representations of the separated components

Component No	***Duration (number of samples)***	***Signal***
1	21	FHSS
2	20	FHSS
3	18	FHSS
4	20	FHSS
5	108	IEEE 802.11b
6	112	IEEE 802.11b
7	102	IEEE 802.11b

Table 3: The MSEs between original and reconstructed eigenvectors, for 45% of the available samples

Component No	***MSE***
1	0.0103
2	0.0087
3	0.0077
4	0.0122
5	$2.3406*10^{-4}$
6	$3.06781*10^{-4}$
7	$2.5467*10^{-4}$

Noisy signal case:

In the sequel, the performance of the decomposition procedure in the noisy environment is considered in terms of the number of extracted eigenvectors (that correspond to the signal components) from noisy signal. It is assumed that the signal is corrupted by the Gaussian noise. Noise, affecting the signal, is distributed in the time-frequency plane. By using the time-frequency domain to extract eigenvectors belonging solely to the signal components, a certain percent of the noise will be eliminated from the signal.

The results for different signal-to-noise ratio (SNR) are shown in Table 4. The number of extracted components from the total number of components is provided within the Table 4. It is shown that all signal components (i.e. eigenvectors that correspond to the signal components) can be successfully separated if the SNR is above – 4 dB. Number of EVD iterations in this case should be slightly higher than number of signal components (in this case, number of EVD iterations is 8 for the SNR=-3.7823 dB, while the number of signal components is 7).

Table 4: Number of extracted eigenvectors that correspond to the signal components, in the case of noisy signal. Different SNRs are observed

SNR (dB)	*Number of extracted eigenvectors*	*Number of EVD iterations*
-4.6599	5	15
-3.7823	7	8
-2.0454	7	8
-0.3898	7	7
0.4935	7	7
1.9965	7	7

VI. CONCLUSION

The procedure proposed in this paper aims at separation and classification of the signals that belong to two interfering wireless standards. Separation procedure is based on the eigenvalue decomposition approach while for the classification, time-frequency representations of the separated components are observed. Classification is done on the randomly under-sampled separated components. It is shown that more than 50% of the signal samples can be avoided during the transmission, and component can be still recovered with the high accuracy. In order to successfully reconstruct randomly under-sampled components, a suitable sparse domain has to be chosen. Due to the nature of the observed signals, it is shown that HT domain can be used as a sparsification domain for the FHSS modulated signals, while for the DSSS modulated signals the DFT shows to be better choice.

ACKNOWLEDGMENT

This work is supported by the bilateral project Montenegro-China “Compressive sensing and time-frequency analysis with applications”, project grant Ministry of Science (World Bank loan): CS-ICT “New ICT Compressive sensing based trends applied to: multimedia, biomedicine and communications”, and the National Natural Science Foundation of China (61571174).

REFERENCES

[1] Valeri P. Ipatov, “Spread Spectrum and CDMA: Principles and Applications”, *John Wiley & Sons, Ltd*, ISBN: 9780470091784, 2005.

[2] M. Gandetto, M. Guainazzo, C. S. Regazzoni, “Use of Time-Frequency Analysis and Neural Networks for Mode Identification in a Wireless Software-Defined Radio Approach”, *EURASIP Journal on Applied Signal Processing*, Vol. 2004, pp. 1778-1790, 2004.

[3] A. Draganic, I. Orovic, S. Stankovic, "FHSS Signal Characterization Based On The Crossterms Free Time-Frequency Distributions," *2nd Mediterranean Conference on Embedded Computing MECO 2013*, pp. 152-155, June 2013, Montenegro, 2013.

[4] M. Ghavami, L. B. Michael, R. Kohno, "Ultra Wideband Signals and Systems in Communication Engineering", Second Edition, *John Wiley & Sons, Ltd,* ISBN 978-0-470-02763-9 (HB), February 2007.

[5] S. Barbarossa, J. L. Krolok, "Adaptive time-varying cancellation of wideband interferences in spread-spectrum communications based on time-frequency distributions," *IEEE Transactions on Signal Processing*, Vol. 47, No. 4, Apr. 1999, pp. 957-965.

[6] A. Draganic, I. Orovic, S. Stankovic, X. Li, Z. Wang, "Reconstruction and classification of wireless signals based on Compressive Sensing approach," *5th Mediterranean Conference on Embedded Computing*, MECO 2016.

[7] M. G. Di Benedetto, S. Boldrini, C. J. M. Martin, J. R. Diaz, "Automatic network recognition by feature extraction: A case study in the ISM band", *CROWNCOM*, June 2010, pp. 1 – 5.

[8] I. Orovic, S. Stankovic, A. Draganic, "Time-Frequency Analysis and Singular Value Decomposition Applied to the Highly Multicomponent Musical Signals," *Acta Acustica united with Acustica*, Vol. 100, No 1, pp. 93-101(9), 2014.

[9] LJ. Stankovic, T. Thayaparan, M. Dakovic, "Signal Decomposition by Using the S-Method with Application to the Analysis of HF Radar Signals in Sea-Clutter", *IEEE Transactions on Signal Processing*, Vol. 54, No. 11, November 2006, pp. 4332- 4342.

[10] X. Luciani, L. Albera, "Joint Eigenvalue Decomposition of Non-Defective Matrices Based on the LU Factorization With Application to ICA," *IEEE Transactions on Signal Processing*, Vol. 63, No. 17, pp. 4594-4608, September 2015.

[11] S. Stankovic, I. Orovic, N. Zaric, C. Ioana, "Two Dimensional Time-Frequency Analysis based Eigenvalue Decomposition Applied to Image Watermarking," *Multimedia Tools and Applications*, Vol.49, No. 3, pp. 529-543, 2010.

[12] G. Chabriel, M. Kleinsteuber, E. Moreau, H. Shen, P. Tichavsky, A. Yeredor, "Joint Matrices Decompositions and Blind Source Separation: A survey of methods, identification, and applications," *IEEE Signal Processing Magazine*, Vol. 31, No. 3, pp. 34-43, May 2014.

[13] I. Orovic, S. Stankovic, "Time-Frequency-Based Speech Regions Characterization and Eigenvalue Decomposition Applied to Speech Watermarking", *EURASIP Journal on Advances in Signal Processing,* Vol. 2010, Article ID 572748, 10 pages, September 2010.

[14] P. Zhang, Z. Hu, R. C. Qiu, B. M. Sadler, "A Compressed Sensing Based Ultra-Wideband Communication System," *IEEE International Conference on Communications*, 14-18 June 2009.

[15] S. Stankovic, I. Orovic, M. Amin, "L-statistics based Modification of Reconstruction Algorithms for Compressive Sensing in the Presence of Impulse Noise," *Signal Processing*, Vol.93, No.11, pp.2927-2931, 2013.

[16] T. Blumensath, M. E. Davies, "Iterative Thresholding for Sparse Approximations", *Journal of Fourier Analysis and Applications*, Vol. 14, No. 5-6, pp. 629-654, December 2008.

[17] LJ. Stankovic, S. Stankovic, M. Amin, "Missing Samples Analysis in Signals for Applications to L-estimation and Compressive Sensing," *Signal Processing*, Vol. 94, pp. 401-408, January 2014.

[18] S. Stankovic, I. Orovic, LJ. Stankovic, "An Automated Signal Reconstruction Method based on Analysis of Compressive Sensed Signals in Noisy Environment," *Signal Processing*, Vol. 104, pp. 43 - 50, November 2014.

[19] J. A. Tropp, A. C. Gilbert, "Signal Recovery From Random Measurements Via Orthogonal Matching Pursuit," *IEEE Transaction on Information Theory*, Vol. 53, No. 12, pp. 4655–4666, 2007.

[20] D. Needell, J. A. Tropp, "CoSaMP: Iterative signal recovery from incomplete and inaccurate samples," *Applied and Computational Harmonic Analysis*, Vol. 20, No. 3, pp. 301-321, 2009.

[21] I. Orovic, S. Stankovic, "A Class of Highly Concentrated Time-Frequency Distributions Based on the Ambiguity Domain Representation and Complex-Lag Moment," *EURASIP Journal on Advances in Signal Processing*, Vol. 2009, Article ID 935314, 9 pages, 2009.

[22] P. Flandrin, and P. Borgnat, "Time-Frequency Energy Distributions Meet Compressed Sensing," *IEEE Transactions on Signal Processing*, Vol.58, No.6, pp.2974, 2982, June 2010.

[23] M. Brajovic, A. Draganic, I. Orovic, S. Stankovic, "FHSS signal sparsification in the Hermite transform domain," *24th Telecommunications Forum* TELFOR 2016, November 2016, Belgrade, Serbia, 2016.

[24] A. Krylov, D. Korchagin, "Fast Hermite projection method," 3rd *Int. Conference on Image Analysis and Recognition (ICIAR '06)*, Vol. 1, pp. 329–338, Povoa de Varzim, Portugal, September 2006.

[25] S. Stanković, I. Orović, LJ. Stanković, "Compressive Sensing approach in Hermite transform domain," *Mathematical Problems in Engineering*, Vol. 2015, Article ID 286590, 9 pages.

[26] A. Sandryhaila, S. Saba, M. Püschel, J. Kovačević, "Efficient Compression of QRS Complexes Using Hermite Expansion," *IEEE Transactions on Signal Processing*, Vol. 60, No. 2, pp. 947-955, February 2012.

[27] M. Brajovic, I. Orovic, M. Dakovic, S. Stankovic, "On the Parameterization of Hermite Transform with Application to the Compression of QRS Complexes," *Signal Processing*, Vol. 131, February 2017, pp. 113–119.

[28] A. Rasiah, R. Togneri, Y. Attikiouzel, "Modelling 1-D signals using Hermite basis functions," *IEE Proceedings on Vision, Image and Signal Processing*, Vol.144, No.6, pp.345,354, 1997.

[29] "Models, Databases, and Simulation Tools Needed for the Realization of Integrated Computational Materials Engineering", Edited by Steven M. Arnold and Terry T. Wong (Editor), ISBN-10: 1615038310

[30] S. M. Schwartz, "Frequency Hopping Spread Spectrum (FHSS) vs. Direct Sequence Spread Spectrum (DSSS) in Broadband Wireless Access (BWA) and Wireless LAN (WLAN)".